The thermodynamic assessment of the Au–In–Ga system

Ghasemi, Masoomeh; Sundman, Bo; Fries, Suzana; Johansson, Jonas

Published in:
Journal of Alloys and Compounds

2014

The thermodynamic assessment of the Au-In-Ga system

M. Ghasemi[a,*], B. Sundman[b], S. G. Fries[c], J. Johansson[a]

[a]*Solid State Physics, Lund University, Box 118 SE-22100 Lund, Sweden*
[b]*INSTN-CEA Saclay, 91191 Gif sur Yvette, France*
[c]*ICAMS, Interdisciplinary Centre for Advanced Materials Simulation, Ruhr-Universitt Bochum, address, Germany*

Abstract

The Au-In-Ga ternary phase diagram is of importance for understanding the involved thermodynamic processes during the growth of Au-seeded III-V heterostructure nanowires containing In and Ga (e.g. Au-seeded InAs/GaAs nanowires). In this work the Au-In-Ga system has been thermodynamically modeled using the CALPHAD technique based on a recent experimental investigation of the phase equilibria in the system. As a result, a set of self-consistent interaction parameters have been optimized that can reproduce most of the experimental results.

Keywords: Ternary alloy system, Phase diagrams, CALPHAD, Thermodynamic modeling, Thermodynamic calculation.

1. Introduction

There have been considerable attempts towards downscaling of electronic and optoelectronic devices. III-V semiconductor nanowires (NWs) are con-

*Corresponding author
Email addresses: masoomeh.ghasemi@ftf.lth.se (M. Ghasemi), bo.sundman@gmail.com (B. Sundman), suzana.g.fries@ruhr-uni-bochum.de (S. G. Fries), jonas.johansson@ftf.lth.se (J. Johansson)

sidered to be useful structures for future device applications [1, 2]. Therefore it is essential to have an understanding of the optimal growth condition of the NWs. One approach is to develop knowledge of the thermodynamic behavior of the materials systems of interest. In the Vapor-Liquid-Solid (VLS) growth mechanism [3], seed particles (often 20-100 nm Au particles) are dispersed on a crystalline substrate. At elevated temperatures, the precursor materials (e.g. metalorganics) supplied in the gas phase decompose on the particle surface and dissolve in it. When the particle is supersaturated, solid material, contributing the growing NW, begins to crystallize at the interface between the particle and the substrate.

We report on the thermodynamic assessment of the Au-In-Ga ternary system which is useful in the growth of Au-seeded III-V semiconductor heterostructure NWs containing In and Ga from group III [4, 5]. The role of group V elements has been ignored in this first step, since the solubility of the group V elements of our interest (As and P) in Au is negligible. The Au-In-Ga system has been assessed using the CALPHAD technique [6] based on the recent experimental evidence [7], resulting in a complete thermodynamic description.

2. Literature review

2.1. Au-In-Ga

To the best of our knowledge, the only experimental investigation of the Au-In-Ga ternary system was reported by Hoyt and Mota in 1978 [8] and it refers to the Au-rich region. They investigated the dependence of Curie temperature (T_c) on the elastic energy of the Au-In-Ga alloys in the fcc phase

with the fixed composition of gold (92 at.% Au). The lattice parameter of the Au-In-Ga alloys with the varying compositions of In and Ga was measured and the correlation between the lattice parameters and T_c was studied.

Very recently an experimental investigation was published [7] related to an isothermal section of the Au-In-Ga phase diagram at 280 °C using the complementary techniques: Differential Thermal Analysis (DTA), X-Ray Diffraction (XRD), Energy Dispersive X-ray Spectroscopy (EDS) and Scanning Electron Microscopy (SEM). As a result, a previously unknown ternary phase was identified [9] which should be included in the thermodynamic description of this ternary system. The new ternary phase, Au_2InGa_2, with a hexagonal structure belonging to the space group $P6_3/mmc$ melts incongruently at 394 °C. Some level of ternary solubility in the binary phases was also observed [7]; thus showing the need for adding interaction parameters to include solubility terms for the corresponding binary phases.

Since, the Au-In-Ga ternary system has not been thermodynamically assessed, we will here present a thermodynamic model for this ternary system, consistent with the recently published experimental results. As the assessment of the Au-In-Ga ternary system using CALPHAD technique depends on the binary sub-systems, we will review here the thermodynamic assessments of Au-Ga, Au-In and In-Ga binaries available in the literature. Table 1 summarizes the crystal structure information of all solid phases in the Au-In-Ga ternary system. The description of the chosen thermodynamic models as well as the corresponding Gibbs energy functions and the interaction parameters will be explained later.

Table 1: Crystal structure data of all solid phases in the Au-In-Ga ternary system.

Phase	Structure and space group	lattice parameters (nm)	composition range	Ref.
Au-fcc	Cub, *Fm-3m*	Au: $a = 0.4072$	Au-In: $0 - 12.7$ *at.*%In	[10]
			Au-Ga: $0 - 12.4$ *at.*%Ga	[11]
In-tetra	Tet, *I4/mmc*	In: $a = 0.32480$ $c = 0.49480$	In-Ga: $0 - 3.1$ *at.*%Ga	[12]
Ga-Orth	Orth, *Cmca*	Ga: $a = 0.45192$ $b = 0.76586$ $c = 0.45258$	In-Ga: 0 *at.*%In	[12]
$D0_{24}$	Hex, *P6$_3$/mmc*	-	Au-Ga: $12.75 - 14.1$ *at.*%Ga	[13]
			Au-In: $12.0 - 14.3$ *at.*%In	[10]
hcp	Hex, *P6$_3$/mmc*	-	Au-In: $13 - 23$ *at.*%In	[10]
Au_7Ga_2-HT	Hex, *P-62m*	$a = 0.77258$ $c = 0.87413$	Au-Ga: $20.4 - 22.1$ *at.*%Ga	[13]
Au_7Ga_2-LT	Orth, -	-	Au-Ga: $21.5 - 23.2$ *at.*%Ga	[14]
Au_7Ga_3	Orth, -	-	Au-Ga: $29.8 - 31$ *at.*%Ga	[14]
AuGa	Orth, *Pnma*	$a = 0.63971$	Au-Ga:	[13]

		$b = 0.62620$	50 *at.*%Ga	
		$c = 0.34630$	Au-In-Ga:	[7]
			Solubility of about 3.0 *at.*%In	
$AuGa_2$	Cub, *Fm-3m*	$a = 0.60758$	Au-Ga:	[13]
			66.7 *at.*%Ga	
			Au-In-Ga:	[7]
			Solubility of about 5.5 *at.*%In	
Au_4In-HT	Hex, -	-	Au-In:	[10]
			$21.5 - 22.2$ *at.*%In	
Au_4In-LT	Hex, *P-3*	$a = 1.0524$	Au-In:	[10]
		$c = 0.4759$	$21.7 - 22.5$ *at.*%In	
$AuIn_3$	Orth, *Pmmn*	$a = 0.58572$	Au-In:	[10]
		$b = 0.47352$	$24.5 - 25$ *at.*%In	
		$c = 0.51504$		
Au_9In_4	Cub, *P-43m*	$a = 0.9843$	Au-In:	[10]
			$28.8 - 31.4$ *at.*%In	
Au_7In_3	Hex, *P-3*	$a = 1.21$	Au-In:	[10]
		$c = 0.851$	$29.8 - 30.6$ *at.*%In	
Au_3In_2	Hex, *P-3m1*	$a = 0.4538$	Au-In:	[10]
		$c = 0.5659$	$35.3 - 39.5$ *at.*%In	
AuIn	Tri, *aP**	$a = 0.430$	Au-In:	[10]
		$b = 1.059$	$50 - 50.1$ *at.*%In	
		$c = 0.356$	Au-In-Ga:	[7]
		$\alpha = 90.54°$	Solubility of about 4.0 *at.*%Ga	
		$\beta = 90.0°$		
		$\gamma = 90.17°$		
$AuIn_2$	Cub, *Fm-3m*	$a = 0.6515$	Au-In:	[10]
			66.7 *at.*%In	
			Au-In-Ga:	[7]
			Solubility of about 9.5 *at.*%Ga	

Au_2InGa_2	Hex,$P6_3/mmc$	$a = 0.42047$	Au-In-Ga:	[9]
		$c = 1.2967$	40 *at.*%Au,	
			20 *at.*%In	

2.2. Au-Ga

The Au-Ga phase diagram has been experimentally investigated several times. In 1987, Massalski and Okamoto [15] redrew the phase diagram based on prior experimental data, especially the work by Cooke and Hume-Rothery [13]. Later, Mouani et al. [16] re-reviewed the Au-Ga system in the investigation of the Au-Ga-Te ternary system.

The first thermodynamic description of the Au-Ga system using CALPHAD technique [6] was reported by Liu et al. in 2010 [17]. Soon afterwards in 2011, the system was reassessed by Wang et al. [11]. There are differences between the two recent assessments in the modeling of several phases. In the work by Wang et al. [11], Au_7Ga_2-HT and Au_7Ga_2-LT phases are modeled as stoichiometric phases due to narrow homogeneity ranges. Also, the phase transition between Au_7Ga_3-HT and Au_7Ga_3-LT was ignored in the most recent assessment by Wang et al. [11] and both phases were merged to one stoichiometric phase. In addition, the $D0_{24}$ phase was modeled using a substitutional model.

In the present optimization, the thermodynamic description by Wang et al. [11] has been selected due to model compatibility with the phases in the Au-In binary system [10]. The phase diagram calculated by the evaluated parameters in [11] is redrawn in Figure 1.

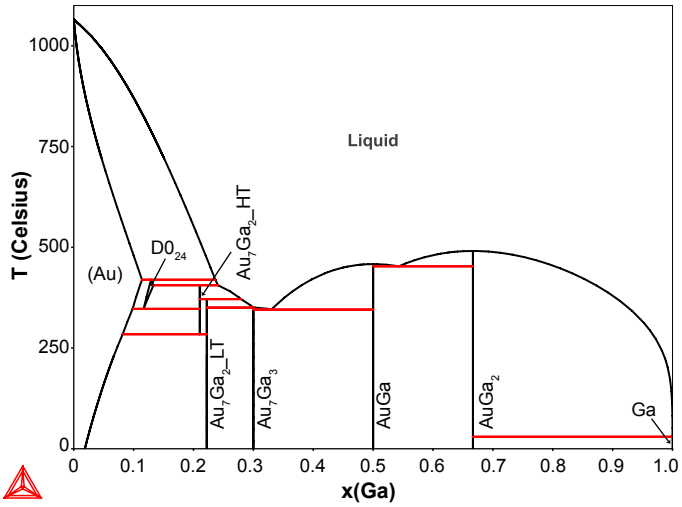

Figure 1: The Au-Ga phase diagram calculated using the parameters assessed by Wang et al. [11].

2.3. Au-In

Based on available experimental data, especially the phase diagram by Massalski [18], Ansara and Nabot presented the first thermodynamic assessment of the Au-In phase diagram in 1988 [19]. In their phase diagram, the $D0_{24}$ phase which is an intermediate phase between fcc and hcp was not included. Furthermore, all intermetallic phases have been considered as stoichiometric phases. Later, in 1992, the system was reassessed by the same authors in the Au-rich side to include the $D0_{24}$ phase [20]. The most recent thermodynamic assessment of the Au-In system was reported by Liu at al. in 2003 [10]. The Au_4In phase was remodeled as two phases: Au_4In-HT and Au_4In-LT to differ between the crystal structures at low and high temperatures. Also, the Au_9In_4 phase has been modeled using a three-sublattice model. Taking the composition range of the Au_3In_2 phase into account, a

three-sublattice model, the same model as for the isotypic Al_3Ni_2 [21] has been adapted for this phase. Moreover, in this assessment, the solubility of In in the fcc phase decreases with temperature at low temperatures which is more realistic than the assessment by Ansara and Nabot [19, 20].

In the present assessment, all parameters evaluated by Liu et al. [10] have been used except for the sub-regular interaction parameter of the fcc phase (${}^1L^{fcc}_{Au,In}$). The lattice stability of the fcc phase for indium was modified in the assessment of the Bi-In-Pb system by Boa and Ansara [22]. However, in the assessment by Liu et al [10], this has not been taken into account and the old unary description of the fcc phase for indium reported by Dinsdale [23] has been used. In the current assessment, the updated SGTE unary descriptions [24] was used. This causes the decomposition of the $D0_{24}$ phase to occur at a higher temperature (26 °C higher) as in the assessment of the Au-In-Sn system by Caccimani et al. [25] which is not in agreement with the experimental value reported by Mikler et al. [26] (See Figure A.8 in Appendix A). Therefore, the ${}^1L^{fcc}_{Au,In}$ parameter was adjusted to reproduce the peritectic formation of the $D0_{24}$ phase at a temperature as close as possible to the experimental results. The Gibbs energies of the phases in the Au-rich corner of the Au-In phase diagram (fcc, $D0_{24}$ and liquid) at 649 °C , the temperature of the invariant reaction: L + fcc $\rightleftarrows$ $D0_{24}$, according to [26], reproduced with the parameters evaluated in the current assessment and with those assessed by Liu et al. [10] have been compared. See Figure A.9 in Appendix A. The calculated Au-In phase diagram is shown in Figure 2.

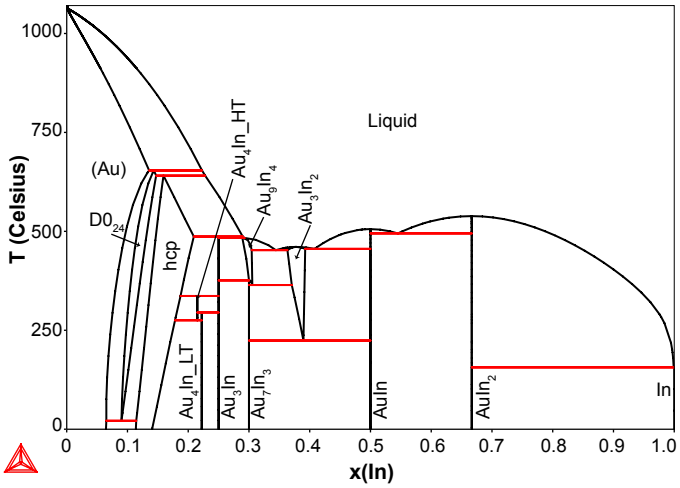

Figure 2: The Au-In phase diagram calculated using the binary interaction parameters (except for ${}^1L^{fcc}_{Au,In}$) assessed by Liu et al. [10] and the modified subregular interaction parameter of the fcc phase in our assessment.

2.4. In-Ga

The In-Ga binary system is a eutectic system with negligible solubility of In in Ga and a limited solubility of up to 2.3 at.% Ga in In. The eutectic reaction occurs at 15.3 °C at 14.2 at.% In [12].

Since the first phase equilibria study on the In-Ga system by Biosbaudran in 1885 [27] and the complete liquidus measurements of the system by French et al. in 1937 [28], the system has been critically assessed several times [12, 29, 30, 31, 32, 33]. Rugg and Chart [32] and Anderson and Ansara [12] thoroughly assessed the system using available liquidus data, enthalpies of mixing, activity measurements and new unary data at about the same time to provide a complete and simple thermodynamic description of the system. While both descriptions were not noticeably different, that of

Anderson and Ansara also included the metastable phase diagram. Later, in 1993, Ravindra and Hajra [33] recalculated the system using complex multi-parameter equations to describe the excess Gibbs energy terms. The description was able to interpret the phase equilibria as well as the high and low temperature data in the system. Nevertheless we used the description by Anderson and Ansara [12] in this assessment because it provides a simpler thermodynamic description with less fitting parameters (Figure 3).

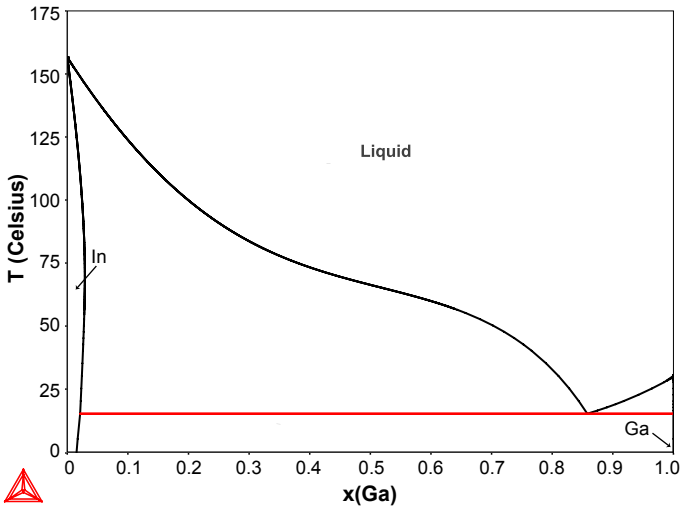

Figure 3: The In-Ga phase diagram calculated using the parameters assessed by Anderson and Ansara [12].

In summary, for thermodynamic assessment of the Au-In-Ga ternary system, the descriptions of Au-Ga, Au-In and In-Ga binary sub-systems have been selected from [11], [10] and [12], respectively. The only exception was that we modified the description of the fcc phase in the Au-In binary system which was not consistent with the updated description of the fcc phase for

pure In in the SGTE database [24].

3. Thermodynamic modeling

The thermodynamic models of the unary, solution and binary and ternary intermetallic phases in the Au-In-Ga ternary system will be briefly discussed here. The adapted models for all solid phases as well as their crystal structure data are summarized in Table 1.

3.1. Pure elements

The temperature dependence of the molar Gibbs energy of pure elements, ${}^0G_m^\theta(T)$, in the phase θ referred to its reference state is described by:

$$\begin{aligned} {}^0G_m^\theta(T) &= G_m^\theta(T) - H^{SER} \\ &= a + bT + cT\ln(T) + dT^2 + eT^3 + fT^{-1} + gT^7 + hT^{-9} \end{aligned} \quad (1)$$

where G_m^θ is the Gibbs energy of the element in the phase θ and H^{SER} refers to the molar enthalpy of formation of the element m at its standard reference state (its stable form at 298.15 K and 1 bar). The empirical parameters a to h for m = Au, In and Ga have been taken from SGTE (Scientific Group Thermodata Europe) thermodynamic database [24].

3.2. Solution phases

There are four substitutional solution phases: liquid, fcc, $D0_{24}$ and hcp in the Au-In-Ga ternary system, which are modeled by only one sublattice.

The Gibbs energy of the binary solution phases is described by:

$$G^{\theta} = \sum_{m=A,B} x_m {}^0G_m^{\theta} + RT \sum_{m=A,B} x_m \ln(x_m) + x_A x_B \sum_{i=0,1} {}^{(i)}L_{A,B}^{\theta}(x_A - x_B)^i \tag{2}$$

where ${}^0G_m^{\theta}$ is the Gibbs energy of the pure element m and x_m is the molar fraction of the element. ${}^{(i)}L_{A,B}^{\theta}$ is the interaction parameter for the phase θ which is expressed as:

$${}^{(i)}L_{A,B}^{\theta} = a_0^{\theta} + a_1^{\theta}T + a_2^{\theta}T\ln(T) \tag{3}$$

where a_0, a_1 and a_2 are parameters to be optimized. In the case of ternary solution phases, the Gibbs energy based on Muggianu extrapolation formula for the excess Gibbs energy terms [34] is described by:

$$\begin{aligned} G^{\theta} = & \sum_{m=A,B} x_m {}^0G_m^{\theta} + RT \sum_{m=A,B,C} x_m \ln(x_m) \\ & + x_A x_B \sum_{i=0,1} {}^{(i)}L_{A,B}^{\theta}(x_A - x_B)^i \\ & + x_B x_C \sum_{i=0,1} {}^{(i)}L_{B,C}^{\theta}(x_B - x_C)^i \\ & + x_A x_C \sum_{i=0,1} {}^{(i)}L_{A,C}^{\theta}(x_A - x_C)^i \\ & + x_A x_B x_C (x_A {}^{(0)}L_{A,B,C}^{\theta} + x_B {}^{(1)}L_{A,B,C}^{\theta} + x_C {}^{(2)}L_{A,B,C}^{\theta}) \end{aligned} \tag{4}$$

where ${}^{(i)}L_{A,B,C}^{\theta}$ ($i = 0, 1, 2$) are parameters to be assessed and are represented by the same kind of equation as in Eq. 3. In this work, only the ternary interaction parameter for the liquid phase was optimized and those for other ternary solution phases were set to zero for simplicity [35].

3.3. Intermetalic compounds

Gibbs energy of the stoichiometric compounds was modeled with two and three sublattices depending on the number of phase constituents. The binary phases with no ternary solubility including Au_7Ga_3, Au_7Ga_2-LT, Au_7Ga_2-HT, Au_7In_3, Au_3In, Au_4In-LT and Au_4In-HT were modeled as:

$$G^{A_aB_b} = a^0G_A^{ref} + b^0G_B^{ref} + L_{A:B}^{A_aB_b} \tag{5}$$

where a and b are stoichiometric coefficients of the compound A_aB_b. The interaction parameters, $L_{A:B}^{A_aB_b}$, has the same form as in Eq. 3 and were directly taken from binary descriptions. The ternary phase, Au_2InGa_2, was modeled with three sublattice as $(Au)_{2/5}(In)_{1/5}(Ga)_{2/5}$ with no mixing of the second element on sublattices.

For stoichiometric binary phases with some level of solubility of In or Ga, mixing of the third element on the second sublattice was taken into account. AuIn and AuGa phases with different crystal structure were modeled as two different phases with mixing of In and Ga on the second sublattice: $(Au)_{1/2}(In,Ga)_{1/2}$, $(Au)_{1/2}(Ga,In)_{1/2}$, respectively, while $AuIn_2$ and $AuGa_2$ phases with the same crystal structure were modeled as one phase: $(Au)_{1/3}(In,Ga)_{2/3}$. The Gibbs energy for these phases was described as:

$$\begin{aligned} G^{A_a(B,C)_b} = {} & a^0G_A^{ref} + b^0G_B^{ref} + L_{A:B}^{A_aB_b} \\ & + a^0G_A^{ref} + b^0G_C^{ref} + L_{A:C}^{A_aC_b} \\ & + L_{A:B,C}^{A_a(B,C)_b} \end{aligned} \tag{6}$$

where for AuIn and AuGa phases, $L_{A:B}^{A_aB_b}$ and $L_{A:B,C}^{A_a(B,C)_b}$ are defined by the same expression as in Eq. 3. To make the AuIn (AuGa) phase unstable on the AuGa (AuIn) side, a large positive value was assigned to $L_{A:C}^{A_aC_b}$. In the

case of $AuIn_2$ and $AuGa_2$, all interaction parameters had the same form as in Eq. 3.

Ordered solid solutions were modeled by three sublattices with partial occupancy of Au and In on the second sublattice. No ternary solubility was taken into account for these phases. Au_3In_2 with similar structure type as Al_3Ni_2 was modeled as $(Au)_{1/2}(Au,In)_{1/3}(In)_{1/6}$, while an $(Au)_{9/13}(Au,In)_{3/13}(In)_{1/13}$ model was used for the Au_9In_4 phase which is isostructural with Cu_9Al_4.

4. Thermodynamic optimization

The thermodynamic descriptions of the constituting binary phase diagrams in the Au-In-Ga ternary system have been taken from the literature. The Au-Ga binary phase diagram studied by Wang et al. [11] has been used. In the case of Au-In binary system, the thermodynamic assessment by Liu et al. [10] has been taken; except for a modification in the fcc phase which was outlined in section 2.3. The In-Ga description has been adapted from the assessment by Anderson and Ansara [12].

The extrapolated ternary phase diagram was optimized using the experimental results with the PARROT optimizer [6, 36, 37] included in the Thermo-Calc software [38]. The ternary solubility was taken into account for those phases that showed noticeable amount of solubility and where enough experimental evidence was available. The thermodynamic description of the new ternary phase, Au_2InGa_2, was also added to the system. Moreover, the ternary interaction parameter for the liquid phase was evaluated. In conclusion, the optimization resulted in a self-consistent set of interaction parameters for the Au-In-Ga ternary system with which most of the experimental

results can be reproduced.

5. Results and discussion

The Gibbs energy functions and the interaction parameters of all phases in the Au-In-Ga and the constituting binaries are given in Table 2. In this work, the ternary interaction parameter (T-independent) for the liquid phase has been optimized. Also, the ternary solubility for AuIn, AuGa, $AuIn_2$ and $AuGa_2$ phases has been taken into account. $AuIn_2$ and $AuGa_2$ constitute one phase with the name of AuX_2, because they have the same crystal structure, meaning that In and Ga mix on the second sublattice. For the fcc, hcp and $D0_{24}$ phases, a large positive value has been assigned to the regular interaction parameter to make these phases metastable on binaries where the elements are unstable in these structures [37]. Moreover, a three-sublattice model has been adapted for the new ternary phase with no binary mixing of the elements on the sublattices.

Table 2: Gibbs energy functions and interaction parameters of the Au-In-Ga ternary system. ${}^0G_x^\theta$ Gibbs energies are taken from the SGTE unary database [24].

Phase and sublattice model	Thermodynamic parameters	Reference
Liquid(Au,In,Ga)	${}^0L_{Au,Ga} = -71830.123 + 42.286T - 4.289Tln(T)$	[11]
	${}^1L_{Au,Ga} = -22892.323 + 5.069T$	
	${}^2L_{Au,Ga} = -8839.911 + 7.674T$	
	${}^0L_{Au,In} = -76196.19 + 64.2914T - 6.6375Tln(T)$	[10]
	${}^1L_{Au,In} = -31134.02 + 81.3582T - 8.5134Tln(T)$	
	${}^0L_{In,Ga} = 4450 + 1.19185T$	[12]

	${}^1L_{In,Ga} = +0.259T$	
	${}^0L_{Au,In,Ga} = +20500$	This work
Au-fcc(Au,In,Ga)	${}^0L_{Au,Ga} = -31511.768 - 12.788T$	[11]
	${}^1L_{Au,Ga} = -20073.352 + 14.067T$	
	${}^0L_{Au,In} = -48493.65 + 46.6237T - 6.8308Tln(T)$	[10]
	${}^1L_{Au,In} = +200$	This work
	${}^0L_{In,Ga} = +25000$	This work
In-tetragonal (In,Ga)	${}^0L_{In,Ga} = +9000$	[12]
Ga-orthorhombic(Ga,In)	${}^0L_{In,Ga} = 0$	[12]
$D0_{24}$(Au,In,Ga)	${}^0L_{Au,Ga} = -41291.692 - 0.227T$	[11]
	${}^1L_{Au,Ga} = -15367.206 - 3.768T$	
	${}^0L_{Au,In} = -48238.66 + 5.3551T$	[10]
	${}^1L_{Au,In} = -48.36 - 16.7932T$	
	${}^0L_{In,Ga} = +25000$	This work
hcp(Au,In,Ga)	${}^0L_{Au,In} = -55780.55 + 13.8198T$	[10]
	${}^1L_{Au,In} = +6788.95 - 32.893T$	
	${}^0L_{Au,Ga} = +25000$	This work
	${}^0L_{In,Ga} = +25000$	This work
Au_7Ga_2-HT: $(Au)_{0.7895}(Ga)_{0.2105}$	$G_{Au:Ga} = -11148.55 - 1.257T + 0.789476{}^0G^{fcc}_{Au} + 0.210526{}^0G^{ort}_{Ga}$	[11]
Au_7Ga_2-LT: $(Au)_{0.7777}(Ga)_{0.2223}$	$G_{Au:Ga} = -12640.544 + 0.326T + 0.777773{}^0G^{fcc}_{Au} + 0.222227{}^0G^{ort}_{Ga}$	[11]
Au_7Ga_3: $(Au)_{0.7}(Ga)_{0.3}$	$G_{Au:Ga} = -16720.107 + 2.397T + 0.7{}^0G^{fcc}_{Au} + 0.3{}^0G^{ort}_{Ga}$	[11]
AuGa: $(Au)_{0.5}(Ga,In)_{0.5}$	$G_{Au:Ga} = -24002.418 + 4.422T + 0.5{}^0G^{fcc}_{Au} + 0.5{}^0G^{ort}_{Ga}$	[11]
	$G_{Au:In} = +20000 + 0.5{}^0G^{fcc}_{Au} + 0.5{}^0G^{tet}_{In}$	This work
	${}^0L_{Au:Ga,In} = -37500$	This work

AuX_2:	$G_{Au:Ga} = -24823.663 + 5.961T + 0.33333{}^0G_{Au}^{fcc} +$	[11]
$(Au)_{0.33333}(Ga,In)_{0.66667}$	$0.66667{}^0G_{Ga}^{ort}$	
	$G_{Au:In} = -26129.06 + 11.1133T + 0.33333{}^0G_{Au}^{fcc} +$	[10]
	$0.66667{}^0G_{In}^{tet}$	
	${}^0L_{Au:Ga,In} = +8900$	This work
Au_4In-HT:	$G_{Au:In} = -8980.42 - 3.3042T + 0.785{}^0G_{Au}^{fcc} +$	[10]
$(Au)_{0.785}(In)_{0.215}$	$0.215{}^0G_{In}^{tet}$	
Au_4In-LT:	$G_{Au:In} = -9382.52 - 3.1015T + 0.778{}^0G_{Au}^{fcc} +$	[10]
$(Au)_{0.778}(In)_{0.222}$	$0.222{}^0G_{In}^{tet}$	
Au_3In: $(Au)_{0.75}(In)_{0.25}$	$G_{Au:In} = -10582.67 - 2.9323T + 0.75{}^0G_{Au}^{fcc} +$	[10]
	$0.25{}^0G_{In}^{tet}$	
Au_9In_4: $(Au)_{0.69231}$	$G_{Au:Au:In} = -2830.47 - 2.5191T + 0.92398{}^0G_{Au}^{fcc} +$	[10]
$(Au,In)_{0.23077}(In)_{0.07692}$	$0.07692{}^0G_{In}^{tet}$	
	$G_{Au:In:In} = -11992.16 - 3.6511T +$	
	$0.69231{}^0G_{Au}^{fcc} + 0.30769{}^0G_{In}^{tet}$	
	${}^0L_{Au:Au,In:In} = +2144.6$	
Au_7In_3: $(Au)_{0.7}(In)_{0.3}$	$G_{Au:In} = -12813.11 - 2.0538T + 0.7{}^0G_{Au}^{fcc} +$	[10]
	$0.3{}^0G_{In}^{tet}$	
Au_3In_2:	$G_{Au:Au:In} = +2153.38 - 8.039T + 0.83333{}^0G_{Au}^{fcc} +$	[10]
$(Au)_{0.5}(Au,In)_{0.3333}$	$0.16667{}^0G_{In}^{tet}$	
$(In)_{0.1667}$		
	$G_{Au:In:In} = -18225.14 + 3T + 0.5{}^0G_{Au}^{fcc} + 0.5{}^0G_{In}^{tet}$	
	${}^0L_{Au:Au,In:In} = -15683.16$	
AuIn:	$G_{Au:In} = -20188.37 + 2.3786T + 0.5{}^0G_{Au}^{fcc} +$	[10]
$(Au)_{0.5}(In,Ga)_{0.5}$	$0.5{}^0G_{In}^{tet}$	
	$G_{Au:Ga} = +20000 + 0.5{}^0G_{Au}^{fcc} + 0.5{}^0G_{Ga}^{ort}$	This work
	${}^0L_{Au:In:Ga} = +39500$	This work
Au_2InGa_2:	$G_{Au:In:Ga} = -35900 + 22.5T + 0.4{}^0G_{Au}^{fcc} +$	This work
$(Au)_{0.4}(In)_{0.2}(Ga)_{0.4}$	$0.2{}^0G_{In}^{tet} + 0.4{}^0G_{Ga}^{ort}$	

Calculated monovariant lines with liquidus projections every 20 °C superimposed with the experimental liquidus temperatures are shown in Figure 4. While a fairly good agreement for most temperatures can be noticed, there are discrepancies between the calculated and the measured temperatures in some cases; especially for liquidus temperatures at 389 °C and 419 °C at gold composition of about 54 at.% and 68 at.%, respectively.

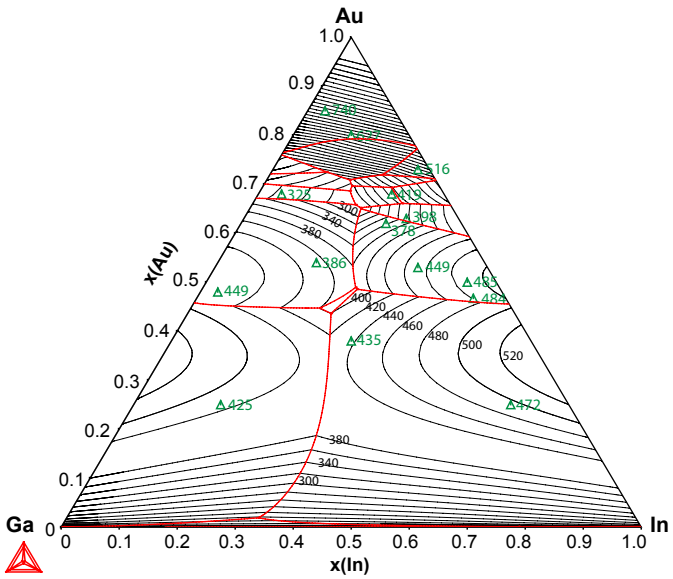

Figure 4: Calculated monovariant lines (in red) of the Au-In-Ga system along with isothermal liquidus projections with 20 °C temperature increments (in black) based on the present work. The calculated liquidus temperatures (°C) are compared to experimental liquidus temperatures (green triangles).

Figure 5 shows the calculated liquidus monovariant lines and the primary crystallization fields. The reaction labels are consistent with the calculated

invariant reactions listed in Table 3. A calculated isothermal section at 280 °C in which all three-phase fields are marked is shown in Figure 6.

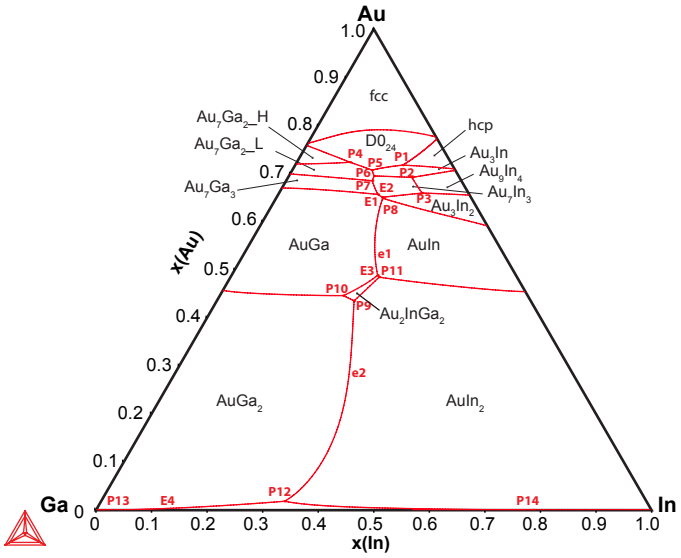

Figure 5: The Au-In-Ga monovariant lines calculated in this optimization. The invariant reactions are labeled according to the reactions in Table 3.

Two vertical sections of the Au-In-Ga phase diagram are shown in Figures 7-a and -b at x(Au)-2x(In)=0 and x(In)-x(Ga)=0.01, respectively. Two Scheil solidification simulations of compositions 1 and 2 (marked on the isoplethal sections in a and b, respectively) are shown in Figures 7-c and -d. The measured temperatures on heating and cooling with the DTA technique have been compared to the calculated temperatures in the isopleths. The predicted temperatures by Scheil simulations for the two compositions are marked with circles on the isopleths. The Scheil simulations are in a good agreement with the calculated vertical sections. This is however expected because equilibrium conditions are not always met in thermal analysis mea-

Table 3: Calculated invariant reactions involving the liquid phase in the Au-In-Ga ternary system. With P type, the ternary and quasi-ternary peritectic reactions are meant. With E type, the ternary eutectic reactions are meant.

Reaction	**T($^\circ C$)**	**Type**	**Composition of liquid**		
			x_{Au}	x_{Ga}	x_{In}
L+hcp $\rightarrow$ Au_3In + $D0_{24}$	398	P1	0.7181	0.0884	0.1935
L + Au_9In_4 $\rightarrow$ Au_3In + Au_7In_3	376	P2	0.6924	0.0847	0.2228
L + Au_9In_4 + Au_7In_3 $\rightarrow$ Au_3In_2	364	P3	0.6600	0.0823	0.2577
L + Au_7Ga_2-HT $\rightarrow$ $D0_{24}$ + Au_7Ga_2-LT	340	P4	0.7240	0.1803	0.0957
L + $D0_{24}$ $\rightarrow$ Au_3In + Au_7Ga_2-LT	307	P5	0.7078	0.1490	0.1432
L + Au_7Ga_2-LT + Au_3In $\rightarrow$ Au_7In_3	293	P6	0.6954	0.1515	0.1531
L + Au_7Ga_2-LT $\rightarrow$ Au_7In_3 + Au_7Ga_3	284	P7	0.6856	0.1596	0.1548
L + AuIn $\rightarrow$ Au_3In_2 + AuGa	276	P8	0.6492	0.1590	0.1918
L $\rightarrow$ Au_7In_3 + Au_3In_2 + AuGa	274	E1	0.6511	0.1588	0.1901
L $\rightarrow$ Au_7In_3 + Au_7Ga_3 + AuGa	272	E2	0.6572	0.1637	0.1791
L + $AuGa_2$ + $AuIn_2$ $\rightarrow$ Au_2InGa_2	400	P9	0.4368	0.3168	0.2494
L + $AuIn_2$ + Au_2InGa_2 $\rightarrow$ AuGa	399	P10	0.4466	0.3295	0.2239
L + $AuIn_2$ + Au_2InGa_2 $\rightarrow$ AuIn	385	P11	0.4851	0.2481	0.2668
L $\rightarrow$ Au_2InGa_2 + AuIn + AuGa	384	E3	0.4879	0.2486	0.2635
L + Au_2InGa_2 $\rightarrow$ $AuGa_2$+ $AuIn_2$	192	P12	0.0179	0.6524	0.3297
L + (Ga) $\rightarrow$ Au_2InGa_2 + $AuGa_2$	290	P13	~ 0	0.9947	0.0053
L $\rightarrow$ Au_2InGa_2 + (In) + (Ga)	152	E4	~ 0	0.8571	0.1429
L + (In) $\rightarrow$ Au_2InGa_2 + $AuGa_2$	96	P14	0.0004	0.2140	0.7856

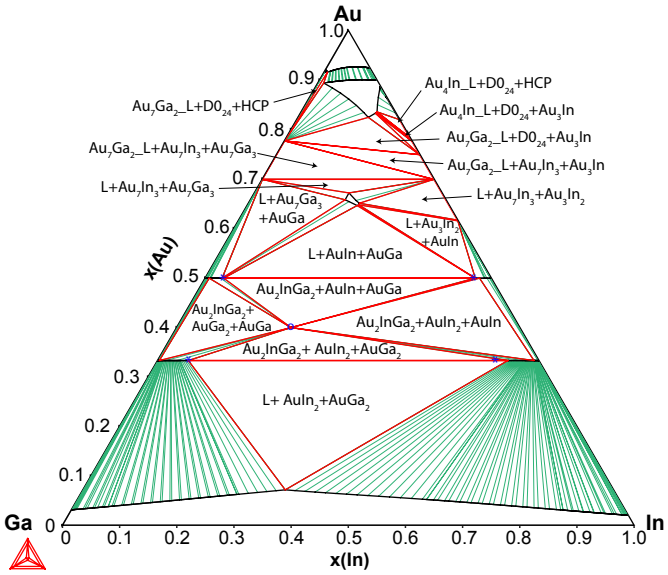

Figure 6: A calculated isothermal section of the Au-In-Ga system at 280 °C based on the present optimization. The three-phase fields are labeled. The asterisk symbols (*) show the measured solubility limits and the circle symbol (o) shows the composition of the ternary phase.

surements. Nevertheless, the discrepancies between the measured and the calculated temperatures point out the need for further experimental investigation of the system.

We present here the first thermodynamic assessment of the Au-In-Ga system. The Au-In-Ga ternary system is comprised of several stoichiometric and non-stoichiometric intermediate phases. It is motivated to perform more experimental investigations of the system for multiple reasons. It was especially difficult to interpret the experimental data in Au-rich corner because the structures of some phases in the Au-In and Au-Ga binaries either are not completely determined (e.g. Au_7Ga_2-LT, Au_7Ga_3 and Au_4In-LT) or are

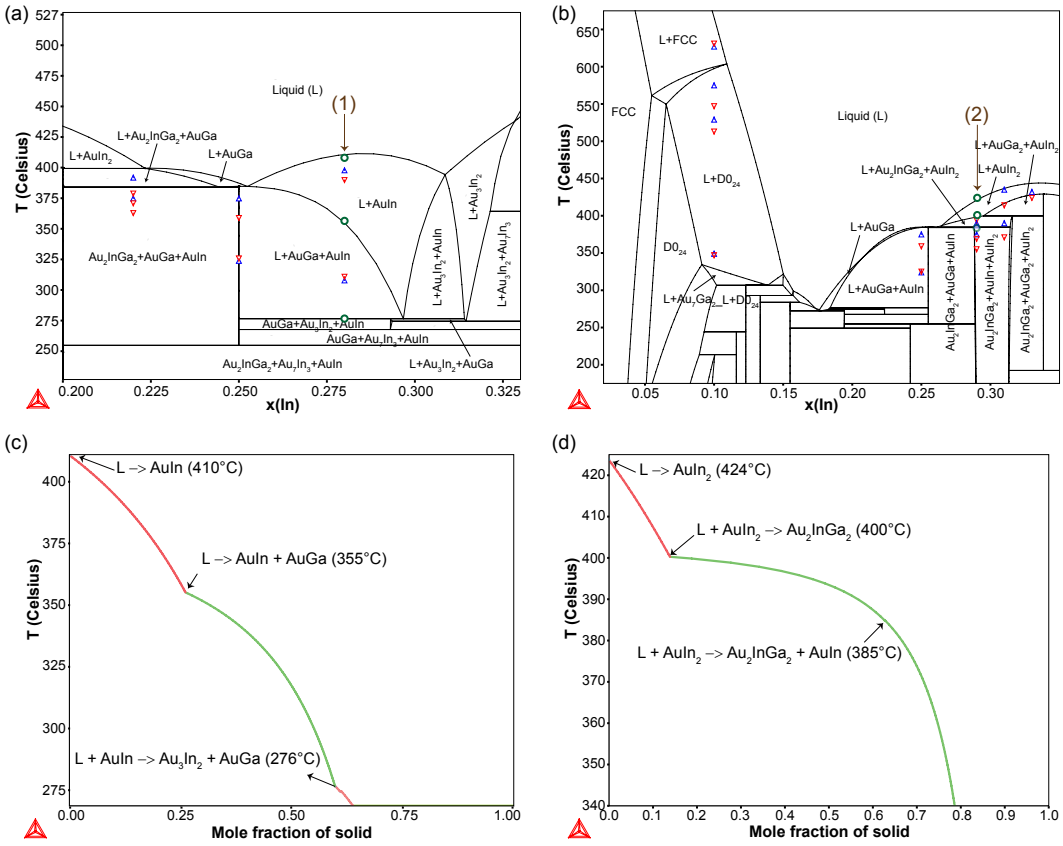

Figure 7: Calculated vertical section of the Au-In-Ga system at (a) x(Au)-2x(In)=0 and (b) x(In)-x(Ga)=0.01 compared to the experimental temperatures determined by the DTA analysis. (c) The Scheil solidification simulation for a sample with composition 1 (56 at.% Au-28 at.% In-18 at.% Ga) marked on the isopleth in part a. (d) The Scheil solidification simulation for a sample with composition 2 (42 at.% Au-29 at.% In-29 at.% Ga) marked on the isopleth in part b. The registered temperatures on heating and cooling are denoted by the upside triangles (in blue) and the downside triangles (in red), respectively. The hollow circles (in green) on the isopleths show the predicted temperatures by Scheil simulations.

highly complex to model (e.g. AuIn, Au_3In_2 and Au_9In_4). On the other hand, some phases in these binaries have similar structures (e.g. Au_4In-LT and Au_4In-HT), creating overlapping diffraction patterns or non-distinguishable microstructural patterns. Another important fact is that it is already known that the In and Ga liquid alloys tend to easily undercool, demanding a long time to reach equilibrium [12]. Therefore the determination of liquidus temperatures in systems containing Ga and In is difficult.

6. Conclusion

The thermodynamic assessment of the Au-In-Ga ternary system based on recent experimental investigations of the system has been carried out. The assessment resulted in a set of complete interaction parameters, which can reproduce most of the experimental results with a good agreement. However, the need for more experimental investigations, especially in the determination of liquidus and phase transition temperatures, to obtain a complete thermodynamic description is outlined.

Acknowledgement

We gratefully acknowledge financial support from the Nanometer Structure Consortium at Lund University (nmC@LU), the Swedish Research Council (VR), and the Knut and Alice Wallenberg Foundation (KAW).

[1] L. Wernersson, C. Thelander, E. Lind, L. Samuelson, III-V nanowires–extending a narrowing road, P IEEE 98 (12) (2010) 2047–2060.

[2] R. Yan, D. Gargas, P. Yang, Nanowire photonics, Nat Photonics 3 (10) (2009) 569–576.

[3] R. S. Wagner, W. C. Ellis, Vapor-Liquid-Solid mechanism of single crystal growth, Appl. Phys. Lett. 4 (89) (1964) 89–90.

[4] K. A. Dick, J. Bolinsson, B. M. Borg, J. Johansson, Controlling the abruptness of axial heterojunctions in III-V nanowires: Beyond the reservoir effect, Nano Lett. 12 (6) (2012) 3200–3206.

[5] S. G. Ghalamestani, M. Ek, M. Ghasemi, P. Caroff, J. Johansson, K. A. Dick, Morphology and composition controlled GaxIn1-xSb nanowires: Understanding ternary antimonide growth, Nanoscale (2014) –doi:10.1039/C3NR05079C.

[6] H. L. Lukas, S. G. Fries, B. Sundman, Computational Thermodynamics: The Calphad Method, Cambridge Uni. press, 2007.

[7] M. Ghasemi, S. Lidin, J. Johansson, The phase equilibria in the Au-In-Ga ternary system, J. Alloys Compd. 588 (2014) 474–480.

[8] R. F. Hoyt, A. C. Mota, Elastic strain energy dependence of Tc in ternary goldbased solid solutions, J. Less Common Met. 62 (1978) 183–188.

[9] M. Ghasemi, S. Lidin, J. Johansson, F. Wang, Bonding in intermetallics

may be deceptive: the case of the new type structure Au2InGa2, Intermetallics 46 (2014) 40–44.

[10] H. Liu, Y. Cui, K. Ishida, Z. Jin, Thermodynamic reassessment of the Au–In binary system, Calphad 27 (1) (2003) 27–37.

[11] J. Wang, Y. Liu, L. Liu, H. Zhou, Z. Jin, Thermodynamic assessment of the Au-Ga binary system, Calphad 35 (2) (2011) 242–248.

[12] T. Anderson, I. Ansara, The Ga–In (Gallium-Indium) system, J. Phase Equilib. 12 (1) (1991) 64–72.

[13] C. Cooke, W. Hume-Rothery, The equilibrium diagram of the system Gold-Gallium, J. Less Common Met. 10 (1) (1966) 42–51.

[14] R. P. Elliot, F. A. Shumnk, TheAu–Ga (Gold-Gallium) system, Bulletin of Alloy Phase Equilibria 2 (1981) 356–358.

[15] T. Massalski, H. Okamoto, Au-Ga (Gold-Gallium), Binary alloy phase diagrams in: American society for metals international, 1987.

[16] D. Mouani, G. Morgant, B. Legendre, Study of the phase equilibria in the ternary Gold-Gallium-Tellurium system, J. Alloys Compd. 226 (12) (1995) 222–231.

[17] L. Jinming, G. Cuiping, L. Changrong, D. Zhenmin, Thermodynamic assessment of the Au-Ga system, J. Alloys Compd. 508 (1) (2010) 62–70.

[18] T. Massalski, H. Okamoto, Au-Ga (gold-Indium), Binary alloy phase diagrams in: American society for metals international, 1987.

[19] I. Ansara, J. Nabot, A thermodynamic assessment of the Au–In system, Thermochim. Acta 129 (1) (1988) 89–97.

[20] I. Ansara, J.-P. Nabot, A thermodynamic re-assessment of the Au–In system in the Au-rich region, Calphad 16 (1) (1992) 13–18.

[21] I. Ansara, N. Dupin, H. L. Lukas, B. Sundman, Thermodynamic assessment of the Al–Ni system, J. Alloys Compd. 247 (12) (1997) 20–30.

[22] D. Boa, I. Ansara, Thermodynamic assessment of the ternary system Bi-In-Pb, Thermochimica Acta 314 (12) (1998) 79 – 86.

[23] A. T. Dinsdale, SGTE data for pure elements, Calphad 15 (4) (1991) 317–425.

[24] SGTE unary database ver. 4.4, Updated from: A. T. Dinsdale, Calphad 15, 1991,317.

[25] G. Cacciamani, G. Borzone, A. Watson, Thermodynamic modelling and assessment of the Au-In-Sn system, Calphad 33 (1) (2009) 100 – 108.

[26] J. Mikler, A. Janitsch, K. L. Komarek, Heat capacity of liquid Au-In alloys, Z. Metallkd. 75 (1984) 719–723.

[27] L. Boisbaudran, Alloys of gallium and indium, C. R. Acad. Sci. 100 (1885) 701–703.

[28] D. J. French, G. W. Saunders, The system Gallium-Indium, J. Phys. Chem. 42 (1937) 265–274.

[29] F. H. Hayes, O. Kubaschewski, A reassessment of the system Indium–Gallium, J. Inst. Met. 97 (1969) 381–383.

[30] M. Rao, W. Tiller, The system In–Ga: Thermodynamics and computed phase equilibria, J. Mat. Sci. 7 (1) (1972) 14–18.

[31] I. Ansara, J. Bros, C. Girard, Thermodynamic analysis of the Ga–In, Al–Ga, Al–In and the Al–Ga–In systems, Calphad 2 (3) (1978) 187–196.

[32] C. R. Bridget, T. G. Chart, A critical assessment of thermodynamic and phase diagram data for the Gallium-Indium system, Calphad 14 (2) (1990) 115–123.

[33] S. R. Reddy, J. P. Hajra, Thermodynamics and phase equilibria in the system Ga-In using multi-parameter functions, Calphad 17 (2) (1993) 151–156.

[34] Y. M. Muggianu, M. Gambino, J. P. Bos, Enthalpies of formation of liquid bismuth-gallium-tin alloys at 723 k. choice of an analytical representation of integral and partial thermodynamic functions of mixing, J. Chim. Phys. 72 (1975) 83–89.

[35] A. Janz, R. Schmid-Fetzer, Impact of ternary parameters, Calphad 29 (1) (2005) 37–39.

[36] B. Sundman, B. Jansson, J.-O. Andersson, The Thermo-Calc databank system, Calphad 9 (2) (1985) 153 – 190.

[37] R. Schmid-Fetzer, D. Andersson, P. Chevalier, L. Eleno, O. Fabrichnaya, U. Kattner, B. Sundman, C. Wang, A. Watson, L. Zabdyr, M. Zinke-

vich, Assessment techniques, database design and software facilities for thermodynamics and diffusion, Calphad 31 (1) (2007) 38–52.

[38] J. Andersson, T. Helander, L. Höglund, P. Shi, B. Sundman, Thermo-Calc & DICTRA, computational tools for materials science, Calphad 26 (2) (2002) 273–312.

Appendix A. Supplementary Information

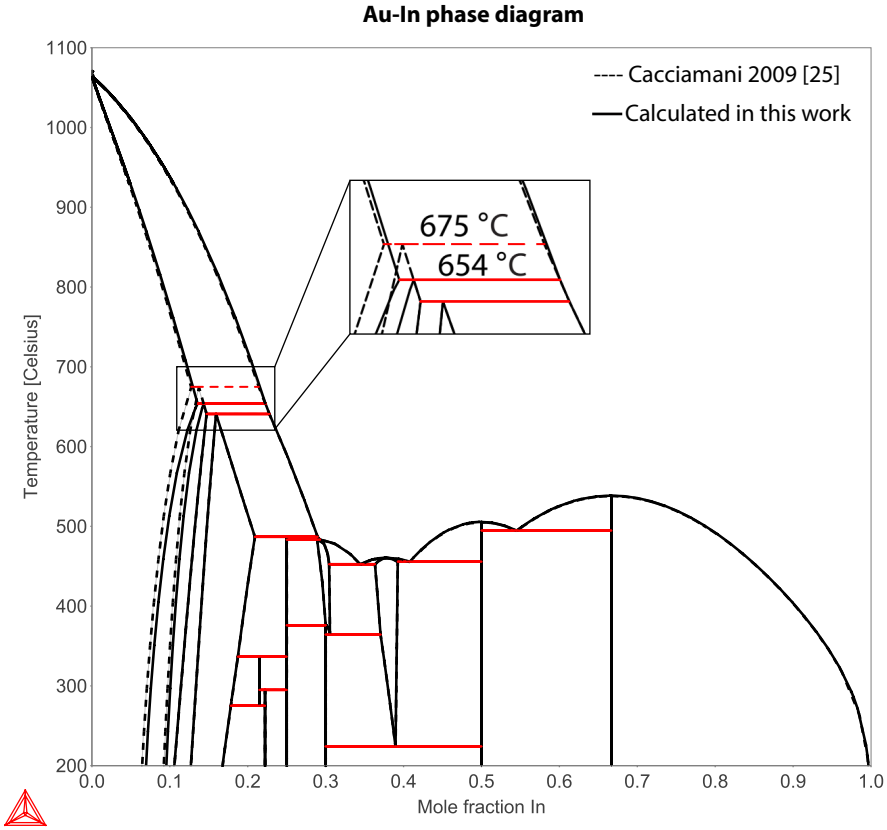

Figure A.8: The Au-In phase diagram calculated in this work (in solid line) is compared with the calculated phase diagram using parameters from Ref. [25] (in dashed line).

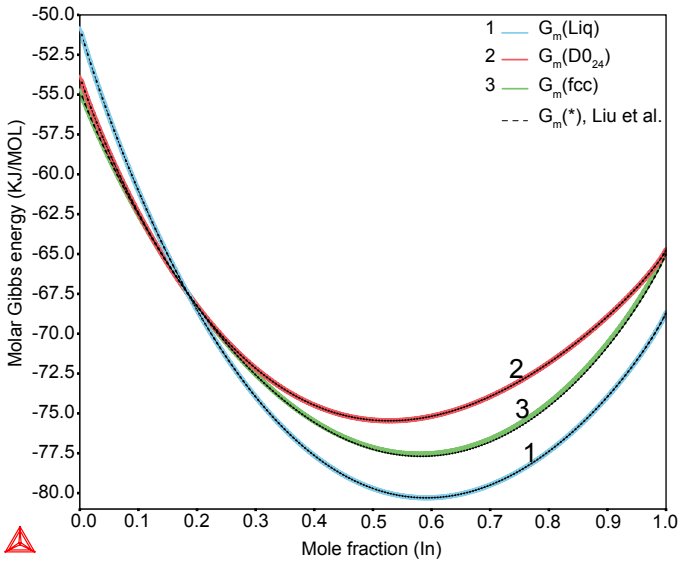

Figure A.9: The calculated Gibbs energies for liquid, fcc and $D0_{24}$ phases reproduced with the parameters evaluated in the current assessment (colored lines) and the parameters assessed in [10] (dashed lines) at 649 °C, the decomposition temperature of the $D0_{24}$ phase.